Investigation of the surface layer formed during the processing of quartz glass using mechanochemical and ionic polishing

© V.M. Zolotarev

ITMO University,
197101 St. Petersburg, Russia,
e-mail: vm-zolotarev@mail.ru

Quantitative studies of the optical parameters of the surface layer formed during the polishing of quartz glass have been carried out. It is shown that the mechanism of formation of the surface layer when using the methods of mechanochemical and ion polishing has much in common. In both cases, the appearance of a surface layer, which differs by a high refractive index from the corresponding bulk properties of glass, is associated with the stress and breaking of the $Si-O-Si$ bridge bonds during hydrolysis during glass polishing. The hydrolysis of $Si-O-Si$ bonds is associated with the formation of $Si-O$ and $Si-OH$ groups, which leads to an increase in the refractive index of the surface layer.

Keywords: surface layer, quartz glass, mechanochemical and ionic polishing, formation of $Si-O$ and $Si-OH$ groups.

Altered layer on the surface of optical elements with properties other than those of the volume, formed during mechanochemical processing (grinding−polishing), affects light transmittance in the UV region and radiation resistance [1–4]. The optical properties of this layer were previously actively studied mainly by the methods of ellipsometry and spectroscopy [5–10]. At present, for these problems, the entire arsenal of modern technical means for monitoring the atomic and molecular composition of defects in the surface layer is widely used [11–17]. The properties of the surface layer of quartz glass altered by mechanochemical polishing (MCP) [18–26] can be improved by subsequent polishing/ion beam bombardment (IBB) [27–35]. As a result, UV light transmission is increased, reflection in IR region is increased, and radiation resistance is noticeably increased [36–38]. Some of the results of these studies concerning the properties of the surface layer are presented in review articles [26–28,33], where various structural and methodological factors (impurities, local structural defects, sample preparation and polishing methods, flatness and surface topography) are considered). Based on a model approach, this work [39] interprets the distribution of the depth and length of cracks in the surface layer formed by the MCM method in terms of key variables, including the abrasive grade and the load on the polishing pad. All of the above features of the MCE process can affect the results of measurements of the optical properties of quartz glass. The character of these variables manifests itself most noticeably in the vicinity of the main UV and IR absorption bands. For quartz glass, the variation in the values of the IR reflection coefficient, which described in the works of various authors, is observed in the ranges of $1250-1000$

and $950-800 \, \text{cm}^{-1}$, which is usually explained by structural defects in the surface layer of the glass [24–27].

The study of physicochemical factors leading to the deviation of optical properties for different methods of surface treatment of quartz glass parts is relevant to reduce the influence of the above factors on the UV light transmission and IR reflection coefficients [16,32–38]. The study of the reasons for causes differences in the measured UV and IR spectra will make it possible to develop ways to optimize the glass processing technology and form a more correct model of a polished surface. This is very important for obtaining reproducible and trustworthy results concerning the properties of optical materials and methods for measuring the properties of thin adsorbed films on the glass surface. Since the adsorbed water films at the interface with the processed optical material (for example, glass) form a system of layers: the external medium−adsorbed layer of molecules−surface altered layer−substrate (glass), than this scheme should be taken into account when studying the characteristics of the surface by different physical methods. With traditional MCP [16,24–28] and IBB [29–39] glass processing methods, depending on the physicochemical conditions of surface formation and material properties, the modified surface layer (SL) of glass and adsorbed layers can introduce significant contribution to the results of measurements of the bulk properties of the material. For example, studies of the water and anhydrous regimes of MCP binary silicate schemes showed that the choice of one or another polishing technological shemeegives a deviation in the measurements of the IR reflection coefficient within $0.015-0.030$, that when using the Kramers-Kronig method,

leads to an error in calculating the optical constants in the range 0.10−0.15 [26].

At the same time, it should be noted that many studies related to the study of SL, as well as adsorbed water films and thin polymer coatings on the surface of polished glass, were carried out by a single-layer model using ellipsometry [5–23], since this method has high sensitivity as applied to the study of thin films. However, in the study of SL, the presence of adsorbed water films on the surface gives an additional phase shift of the light beam, which leads to systemic errors in the calculation of SL parameters in the framework of a single-layer model [21]. Therefore, taking into account the difficulties in extracting physical and chemical information about the structure of an object from ellipsometric measurements in the work [4], it is emphasized that„the refraction index is an important parameter for optical materials, but is not of particular value as a physical and chemical characteristic“. For these proposition, spectroscopy methods are better suited, although they have a lower sensitivity, but they are more informative, as a result of which a greater reliability of the results is achieved The combination of a number of mutually complementary research methods is optimal for studying thin films.

The purpose of this work is a comparative study of the optical and physicochemical properties of a polished surface for the methods of MCP and IBB processing of quartz glass.

Optical model of the object and research methods

As model samples, plates with dimensions of $30 \times 30 \times 5$ mm made of KU-1 quartz glass and K-8 glass were studied. For KU-1 glass, the influence of the choice of technological modes of polishing was studied: abrasive powder, type of emulsion liquid, load on the polishing pad, polishing time, and other parameters.

Typical single-layer optical model of a polished surface with an isotropic SL, used in most works [5–23], is shown in Fig. 1, *a*.

Although modern methods of ellipsometry and spectroscopy make it possible to study the profile shape of the refractive index in SL [18–23,40–46], however, to solve this problem, one has to use more time-consuming methods of multi-angle measurements. The real scheme of the MCP surface is not a single layer and should take into account not only the gradient properties of the SL, but also an additional thin surface layer consisting of adsorbed water and hydroxycarbonates (Fig. 1, *b*). For example, in the work [26] a detailed model of the surface structure of a polished binary glass of formulation: $Na_2O\text{-}SiO_2$ is considered, taking into account microcracks, a layer of silica gel, leached layer and ion exchange layer In the work [38], a model of the structural and morphological structure of the MCP for surface of quartz glass is presented, consisting of a fractured layer (polishing, modified layer or Beilby layer), of a defective layer including oxygen-deficient centers (ODC), non-bridging oxygen hole centers (NBOHC), the oxygen of which is not included in the grid of connections in glass, and nano-sized particles of increased density of unknown nature (Fig. 1, *with*). The layer of adsorbed water was not taken into account in these models. Based on the variety of experimental situations, the details of the optical model of the object (Fig. 1, *b*) are formed by the authors based on the knowledge of the features of the chosen research method, as well as on the basis of the totality of available information about the properties and structure of the surface.

For a transparent isotropic thin film (single-layer model), by measuring the ellipticity Ψ and the phase shift Δ of the reflected light, one can determine the refractive index n_2 and the thickness d of the PS layer (Fig. 1, *a*). When the PS layer thickness is $d \ll \lambda$, the dependence between d and the parameter Ψ is expressed in terms of ratio of the amplitude reflection coefficients r_p and r_s of polarized light. For the Brewster angle, when $\Delta = \pi/2$, the relationship between the parameters d and Ψ is determined from the Drude equation [5]

$$\Psi = \frac{r_p}{r_s} = \frac{\pi}{\lambda} \int_0^d \frac{(\varepsilon_2 - \varepsilon_1)(\varepsilon_2 - \varepsilon_3)}{\varepsilon_2} \, dz, \qquad (1)$$

where ε_1, ε_2, ε_3 are the permittivities of the adjacent media and the PS. Since the function $\varepsilon_2 = n_2^2(z)$ is unknown, practical the averaged value $\varepsilon_2 \cong \varepsilon_{el}$ is usually used, where $\varepsilon_{el} = n_{el}^2$. An assessment of the influence of the choice of model parameters was made in the work [26] for the isotropic and gradient MCP model of the surface of polished glass $33.4 \cdot Na_2O - 66.6 \cdot SiO_2$ and without taking into account the layer of adsorbed water on the surface. The variation between the data for the compared calculation schemes was: for the value of $n_{el} = 1.483$ and $1.474 - 1.505$ (for the glass volume $n = 1.505$), and for the thickness of the PS 800 Å and 1200 Å respectively. It is noted that the deviation of the obtained values of n_{el} from the corresponding value $n = 1.457$ for SiO_2 glass indicates a complex structure of SL. Thus, the magnitude ε_{el} measured in the framework of the one-layer model is effective and characterizes the averaged properties of the PS and adsorbed layers. When the thickness of the adsorbed water layer is much smaller than the PS thickness, in these cases the single-layer model gives quite satisfactory results when studying the PS parameters of polished glasses by ellipsometry. On the contrary, when studying the SL of a metal substrate, the presence of a thin layer of water on the surface significantly affects the results of polarization measurements due to the optical properties of metal and water varies wildly.

To study the structural properties of the surface of dielectrics, it is convenient to use the IR ATR [44] spectroscopy technique, since the spectral absorption regions of SL and adsorbed layers are different In the ATR method, the external medium *1* consists of a transparent highly refraction material, $\varepsilon_1 = n_1^2$ is permittivity (Fig. 1, *b*). The
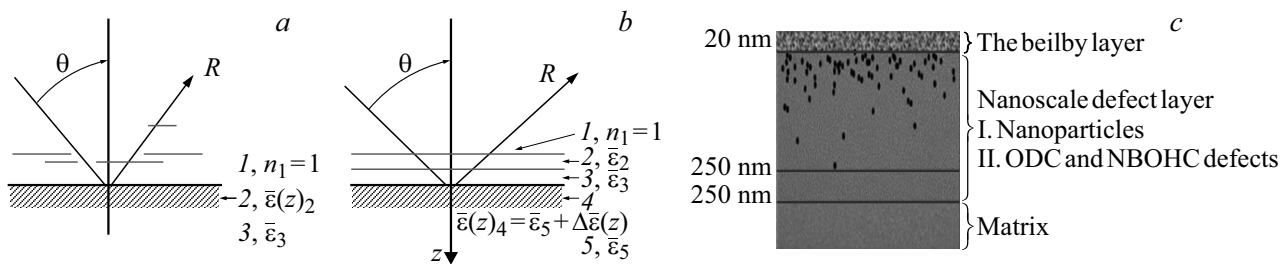
Figure 1. Optical model of a polished surface: a is single-layer system, 1 — environment (n_1 is refraction index), 2 is technologically modified SL ($\bar\varepsilon_2$ is complex permittivity), 3 is substrate ($\bar\varepsilon_3$ is complex permittivity of the substrate); b is multilayer system: 1 is external medium (n_1 is refraction index), 2 is sorbed water film ($\bar\varepsilon_2$ -is complex permittivity), 3 is adsorbed organic film ($\bar\varepsilon_3$ is complex permittivity), 4 its technologically modified SL, ($\bar\varepsilon_4 = \bar\varepsilon_5 + \Delta\bar\varepsilon(z)$ is complex permittivity of SL), 5 is substrate (glass, $\bar\varepsilon_5$ is complex permittivity); c is structural-morphological model of SL of quartz glass for MCP [38]: scale on the right, from top to bottom: Beilby layer, defective layer: 1 are nanoparticles, 2 ODC (oxygen vacancy defects) are oxygen vacancy defects, NBOHC (non-bridging oxygen hole center, matrix is glass thickness.

dielectric properties of the *2, 3* layers of adsorbed water and hydrocarbon molecules, $\bar\varepsilon_{2,3}$, are known [25]: for the region $3800-2800$ cm^{-1} absorption $\varepsilon''_{2,3} \leq 0.3$, and for the region $1300-900$ cm^{-1} (absorption band 1120 cm^{-1} of the bridge Si−O−Si) the value $\varepsilon''_{2,3} \approx 0$. The value of $\bar\varepsilon_4$ for the SL (layer *4*) can be represented under the condition $z \ll \lambda$ in the form of a perturbation of the dielectric properties for the substrate equal to $\bar\varepsilon_4 = \bar\varepsilon_5 + \Delta\bar\varepsilon(z)$, where $\bar\varepsilon_5$ is the complex permittivity $[\bar\varepsilon = \varepsilon' + i\varepsilon'', \varepsilon' = n^2 - k^2, \varepsilon'' = 2nk$, $(\bar n = n + ik)]$ of the studied material in the volume. SL parameters can be found for the case of exponential change in the function $\Delta\bar\varepsilon(z)$. This type of function is typical for diffusion processes that are implemented with typical MCP and IBB methods for processing optical materials [25,33]. The parameters of the function $\Delta\bar\varepsilon(z)$ are determined for three typical cases: *1* i.e. the medium under study is optically transparent, $\varepsilon''_5 = 0$; medium *2* has a weak absorption $\varepsilon''_5 \ll 0.1$, in this case the angles of incidence $\theta > \theta_{cr}$ satisfy the relation $1 - R \ll 1$, where R is reflection coefficient; the medium *3* has absorption $\varepsilon''_5 \gg 0.1$ (general case). This situation is typical when studying in the vicinity of the fundamental absorption bands of dielectrics and oxide films on the surface of metals. The solution to the problem of determining the parameters (thickness d and function $\Delta\bar\varepsilon(z)$) of SL for all three cases is given in the works [40–42].

The first case $\varepsilon''_5 = 0$ is typical for the choice of the SL model of a polished optical material in the water absorption region $\lambda \approx 2.7\,\mu m$, since during the MCP of the material, water molecules that have absorption in this region diffuse at the ?abrasive emulsion material? interface and thereby form special properties of the SL, while the function $\Delta\bar\varepsilon(z)$ changes exponentially . For the case $\varepsilon''_5 = 0$, one can obtain an analytic expression for the width of the transition layer z_0 and the absorption coefficient $\alpha = 4\pi k\nu$ [cm^{-1}] water diffused in the SL layer. The parameters z_0 and α_0 are found by measuring the reflection $R_{1,2}$ at two radiation incidence

angles $\theta_{1,2}$. Transition layer width $z_0 = 1/2q$, where

$$q = \frac{2\pi n_1}{\lambda}\left[\frac{\Delta_1 - \Delta_2}{\gamma - 1} - \Delta_2\right], \qquad (2)$$

$$\Delta_{1,2} = \sqrt{\sin^2_{1,2} - (n_4/n_1)^2}, \quad \gamma = \frac{D_2}{D_1}\frac{\cos\theta_1}{\cos\theta_2}, \qquad (3)$$

where $1 - R^N_{1,2} = ND_{1,2}$, N is number of reflections, $D_{1,2} = -\ln R_{1,2}$ is optical density. Measurements of $\alpha(z)$ and $z_0 \cong d$ were carried out using ATR elements from Ge ($n_1 = 4.0$) and ZnSe ($n_1 = 2.4$) for pairs of angles $\theta = 68° - 73°$.

For the considered case of an exponential change in the function $\alpha(z)$, the absorption coefficient α_0 at the boundary of the SL layer is found from the expression

$$\alpha_0 = \frac{2\pi n_4}{\lambda} D_2 \frac{n^2_{41} - 1}{\cos\theta_2} \frac{\Delta_1 - \Delta_2}{\gamma - 1}. \qquad (4)$$

If the parameters of the function $\alpha(z)$ are known, then the form of the function $C_{OH}(z)$, which characterizes the distribution of hydroxyls in SL, is uniquely determined. The value of $C_{OH}(z = 0)$ can be found from the relation $\alpha_0 = \varepsilon^0 C_{OH}$, where ε^0 is hydroxyl extinction coefficient [l/mol·cm]; the corresponding data are available in Table 1 [25].

The third case, when $\varepsilon''_5 \gg 0.1$, is typical for studies in the region of fundamental absorption bands of the Si−O−Si bond. For the given spectral IR region, taking into account that the thickness of the adsorbed films is $d_{2,3} \ll \lambda$ [42,43], when calculating the parameters $\Delta\bar\varepsilon(z)$ of the SL, which are carried out in the long-wavelength IR range, where $\varepsilon''_{2,3} \approx 0$, the presence of $d_{2,3}$ films can be neglected. It should be noted that there are other methods for calculating the gradient parameters of SL, based on reflection measurements for a number of angles [45,46]. For example, in the paper [45] a method is proposed for finding the gradient parameters of a multilayer system from experimental reflection spectra based on Fresnel's

Table 1. Optical parameters of SL of polished glass KU-1, MCP method

Number of sample	Time of polishing. h	Ellipsometry, $\lambda = 632.8$ nm		Spectroscopy					
		Isotropic layer model		Vacuum UV			IR		
				Experimental data			Gradient layer model		
		External reflection						ATR	
		$N_{el} - 1$	D_{el}, nm	$E_{ev_{max}}$	R_{max}, %	$n - 1$	R_{max}, % $\nu = 1120\,\mathrm{cm}^{-1}$	$\varepsilon' + i\varepsilon''$ $\nu = 1250\,\mathrm{cm}^{-1}$	d, nm
1	0.5	0.432	220	9.7	17.1	0.60	67	65	$-0.94 + i0.88$	180
2	3	0.481	40	9.7	17.3	0.58	71	68	$-0.54 + i0.68$	75
3	6	0.462	20	10.0	19.0	0.52	73.5	71	$-0.27 + i0.54$	19
4 (the cleaved face)	0	0.457	0.0	10.2	18.7	0.46	74	73.5	$-0.13 + i0.4$	0.0

Note. Table values in column $n - 1$ are obtained by integrating $k(\nu)$ in the VUV spectrum; the values of $R_{max}\%$ in the column for $\nu = 1120\,\mathrm{cm}^{-1}$ on the left is data of direct measurements of R, and on the right are calculated from the data of $\varepsilon' + i\varepsilon''$ calculated for SL is gradient layer model.

recursive formulas. This technique for calculating multilayer systems is widely used for the synthesis of interference filters. The method does not cause restrictions on the properties of the layers of the system under study, but requires the input of an interval of values of the desired parameters of the layers, which limits the time of the machine search for the global minimum. This method of calculation was tested in the study in the IR range of the properties of the SL of thermally annealed lead-silicate glass -i.e. material for microchannel plates. These methods are universal, but require significant computational resources, for conventional technical means this leads to a large expenditure of computer time [45,46].

If the function $\Delta\bar{\varepsilon}(z) = \mathrm{const}$ and $\varepsilon''_{2,3,4} < 0.3$, the determination of thickness d for SLs and adsorbed molecular layers for $d_{2,3} \ll \lambda$ in IR spectroscopy is simplified [44], since in the spectral region where the main absorption bands $3800-2800\,\mathrm{cm}^{-1}$ of adsorbed water are and hydrocarbons $\varepsilon''_5 = 0$. Moreover, the absorption frequencies of adsorbed water in the *2* layer (Fig. 1, *b*) differ from the frequencies of water diffused into the *4* layer (SL), which facilitates the separation of different types water and their identification. Since, in the approximation of homogeneous layers *2* and *3*, the values of n and α of these layers are close to the corresponding values of condensed media, in this case the calculations of $d_{2,3}$ are carried out in the approximation of the model of isotropic layers *2, 3* and *4* (Sl) ($n^2_{2,3} = \varepsilon_{2,3}$, $n^2_4 \sim \varepsilon_5$, $k_{2,3,4} < 0.1$). The values of α_2 and α_3 for condensed H_2O and C_xH_y molecules can be find in reference books [47,48], and the value of α_4 for sorbed H_2O molecules can be find i in the work [25]. For the typical case $d_{2,3,4} \ll \lambda$ within the $\varepsilon''_{2,3,4} < 0.3$ approximation for the ATR method and the perpendicular component of the polarized reflection $R_\perp$ you can write an equation

$$1 - R_\perp = D_\perp \approx \alpha_2 \frac{4n_{21}d_2\cos\theta}{1 - n^2_{51}}$$
$$+ \alpha_3 \frac{4n_{31}d_3\cos\theta}{1 - n^2_{51}} + \alpha_4 \frac{4n_{41}d_4\cos\theta}{1 - n^2_{51}}, \quad (5)$$

where $n_{21} = n_2/n_1$, $n_{31} = n_3/n_1$, $n_{41} = n_4/n_1$, $n_{51} = n_5/n_1$ are relative refraction indices, $n_{41} \approx n_{51}$, $\alpha_4 = \varepsilon^0 C_{OH}$, C_{OH} is volume fraction of hydroxyls in SL. The above expression refers to the case when the $\alpha_{2,3,4}$ analytic bands do not overlap or can be separated into individual components. This situation is typical in the study of different types of water molecules, the bands of which partially overlap. For example, to determine the thickness of $d_{2,4}$ layers in the case of quartz glass containing H_2O molecules of different types, it is required to divide the complex contour $D_\perp$ into components $D_{\perp 2}$ and $D_{\perp 4}$, which is achieved using standard fittings. In concluding this section, it can be noted that the optical model (Fig. 1, *b*) agrees in main details with the morphological model of the MCP surface (Fig. 1, *b*), in which, however, does not take into account the absorption layers of water and hydrocarbons.

Discussion of results

Studies of the kinetics of quartz glass polishing by different methods make it possible to reveal some physicochemical features of the polishing process, which have a significant effect on the surface properties. The formation of SLs with properties that differ in thickness and absorption in the layer (depending on the choice of technological modes of polishing) leads to a noticeable deviation of the experimental data, which, for example, is observed when comparing the results of measuring the optical constants of quartz glass (SiO_2) obtained by different authors [26–28].

Mechanochemical polishing

Ellipsometry method

The influence of the technological modes of MCP on the properties of SL has been repeatedly studied by ellipsometry and IR spectroscopy, where the dependence of the refractive index n_{el} of SL on the composition of the polishing abrasive,
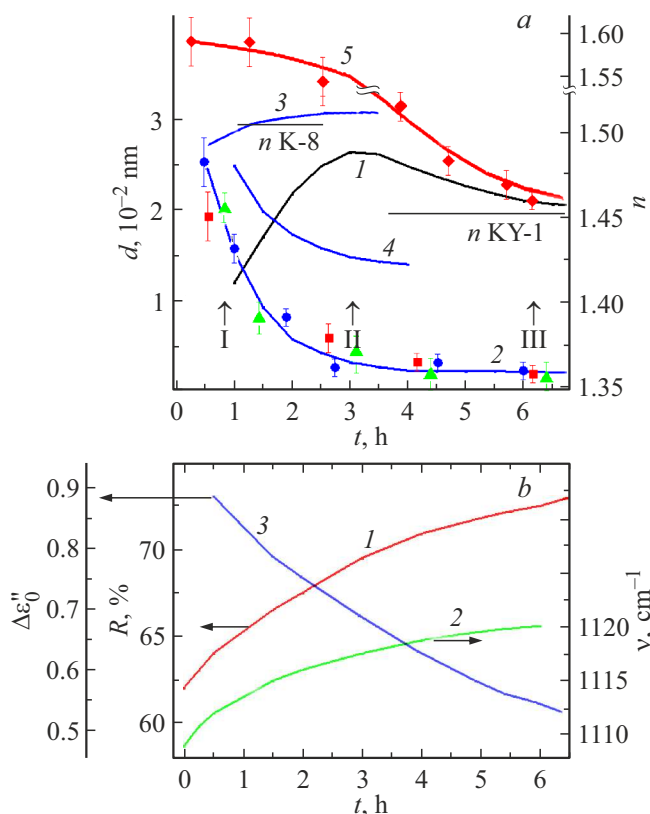
Figure 2. Dependence of the parameters of the SL of glass on the polishing time, the MCP method. a — (ellipsometry, $\lambda = 632.8$ nm) refractive index n_{el}: 1 — KU-1, 3 — K-8; PS thickness d_{el}, nm: 2 — KU-1, 4 — K-8. (VUV spectroscopy): 5 is refraction index, n_{VUV}. Experimental points on the curve 2 (Fig. 2, a): ellipsometry method — •; ATR method, d_{IR} measurements were made in the IR band: ■ — $\lambda = 8\,\mu$m. ▲ — $\lambda \approx 2.7\,\mu$m. b — (IR spectroscopy) 1 — reflection coefficient R ($\nu_{max} = 1120$ cm^{-1}); 2 — band shift $\nu_{max} = 1120$ cm^{-1}; 3 — perturbation $\Delta\varepsilon_0''$ of the imaginary part of the permittivity of the SL in the band $\nu = 1250$ cm^{-1}.

the type of emulsion liquid (for example, water, ethylene glycol), polishing modes and methods [26,32–39]. The dependence of n_{el} on the glass polishing time KU-1 is most clearly seen when diamond powder is used as a polishing abrasive; for softer abrasive powders, this regularity was not observed[1] (Fig. 2, a).

The deviation of n_{el} from the bulk properties of works in a number of papers [16,17] was associated with the introduction of an abrasive into SL, and in other papers [14], with stresses leading to local inhomogeneities in SL. These hypotheses do not take into account the role of the physicochemical processes of the MCP method, since the n_{el} parameter reflects the integral properties that depend, along with the above, on a number of other factors: the chemical structure of SL and the presence of adsorption

---

[1] Ellipsometric measurements were performed at the "RESEARCH AND TECHNOLOGY INSTITUTE OF OPTICAL MATERIAL SCIENCE OF THE ALL-RUSSIAN SCIENTIFIC CENTER" VAVILOV's STATE OPTICAL INSTITUTE by V.I. Pshenitsyn.

films on the surface. It follows from the characteristic shape of the n_{el} curve that the region denoted by the Roman numeral **I** (curve 1, Fig. 2, a) is determined by the total contribution glass microroughnesses KU-1 and the volumetric amount of the adsorbed medium (H_2O and C_xH_y), which refers to the largest thickness of the SL layer, when microelevations from the final grinding stage were removed in the MCP process. For this stage of polishing, the thickness of the adsorbed layers is $d_{2,3} \approx 2-4$ nm, which is much less than the thickness of the SL, i.e. $d_{2,3} \ll d_4$. Region III characterizes the last stage of glass processing KU-1, when the initial SL layer, formed during grinding, decreases during polishing to its minimum value. At the same time, as can be seen from the comparison of the values of n_{H_2O} and $n_{C_xH_y}$, as well as the quantities n_{el}, for the last stage of glass polishing KU-1 (curve 1, Fig. 2, a), the ratio $d_{2,3} < d_4$ is retained (Table 1).

For K-8 glass, the dependence of n_{el} on time for MCP (curve 3, Fig. 2, a) is much weaker than for KU-1, which should be associated with the presence of Na, K, B and other oxides in the glass [24–26]. The presence of these components destroys the glass network and leads to a large set of Si−O−Si bond angles in K-8 glass. These bonds are energetically compensated due to the introduction of Na, K, B, etc. atoms, as well as H_2O molecules located in the volume of the glass. The above arguments are consistent with the larger value of the surface defect layer of the SL for K-8 glass, which is clearly seen from a comparison of the thicknesses d_{el} of KU-1 and K-8 glass (curves 2 and 4, Fig. 2, a). It can be noted that for both types of glasses KU-1 and K-8 the values of n_{el} in region III (Fig. 2, a and Table . 1) more than the reference data [46], which characterize the corresponding properties of these glasses in volume.

VUV spectroscopy method

Independent measurements of the n polished surface KU-1 were performed by vacuum UV reflection spectroscopy [24]. Reflection R in the region $\lambda = 500-2500$ Å was measured in a vacuum chamber, so there was no adsorbed water on the glass surface KU-1 (layers $d_{2,3} \approx 0$, Fig. 1, b), and thus these layers did not affect the measurements R. Then, using the Kramers?Kronig method, the spectrum $k(\lambda)$ was calculated from the spectrum $R(\lambda)$ in the range $\lambda = 500-2500$ ÅThe subsequent integration of the $k(\lambda)$ spectrum made it possible to obtain n SL data for different glass polishing times KU-1. The integration of the spectrum $k(\lambda)$ was performed using the relation

$$\frac{1}{2\pi} \int k(\nu)\, d\ln\nu \approx n - 1. \qquad (6)$$

The dependence of the value of n_{VUV} on the polishing time obtained by the VUV spectroscopy qualitatively agrees with the data of n_{el} ellipsometry, but is characterized by large values of n for the initial stage of polishing (Fig. 2, curves 1 and 5, Table 1). The values of n_{VUV} directly characterize the refraction index n in the visible region of the spectrum.

The dependence of n_{VUV} on the polishing time in regions I and II (curve *5*, Fig. 2, *a*) differs numerically from the corresponding segments of the curve *1*. This is due to the fact that $d_{2,3} \neq 0$ layers are not taken into account when processing ellipsometric measurements, while $d_{2,3} \approx 0$ layers are taken into account for VUV spectroscopy, since the measurements are performed in vacuum. In addition, the features of the interaction of radiation with a gradient surface that is inhomogeneous in thickness are affected by a large difference in the wavelengths of the probing radiation of the compared methods: ellipsometry ($\lambda = 632.8$ nm) and VUV spectroscopy ($\lambda \approx 100$ nm) . Due to the values of $\varepsilon_4^{\nu} \gg 0.1$ for the short-wavelength region of the spectrum, the VUV reflection spectroscopy method characterizes to a greater extent the properties of the outer boundary of the SL. As the thickness (d_4) of the SL decreases during polishing, when the ratio $d_4 \leq \lambda$ is reached, the properties of the substrate (regions II and III) begin to appear in the VUV spectra. As d_4 decreases, the value of n SL for both curves *1* and *5* (Fig. 2, *a*) gradually decreases, but n slightly exceeds the value for the volume of glass. The values of d and n for different polishing times (regions I, II, and III) of KU-1 glass are presented in numerical form in Table 1 for three independent methods. For comparison, Table 1 presents the data of n measurements for the KU-1 cleavage, where the SL is practically absent.

IR spectroscopy method

An additional study of the main factors influencing the formation of R, n, and $\Delta\varepsilon_0''$ SL values during polishing of KU-1 glass was performed using specular reflection spectroscopy and ATR (Fig. 2, *b*). It can be seen from the figure that the influence of different stages of polishing manifests itself in a smooth change in the parameters R and ν of the 1120 cm^{-1} band in the IR spectrum, which is associated with a decrease in the parameter d_4 SL in the MCP process.

The spectral behavior of $\Delta\varepsilon_0''$ was calculated from the IR ATR spectra (Fig. 3) for the vicinity of the 1120 cm^{-1} band. The calculation is made for the case. $\varepsilon_5'' \gg 0.1$ when the function $\Delta\bar{\varepsilon}(z)$ varies exponentially; parameters $d_{2,3} \ll \lambda$, $\varepsilon_{2,3}'' \approx 0$. The specific values of the constants ε_5 and $\varepsilon 5''$ for calculating $\Delta\varepsilon_0''$ were taken from [48]. The results of calculating z_0 and the coefficient $\Delta\varepsilon_0''$ for the imaginary part of the function $\Delta\bar{\varepsilon}(z)$ (1250 cm^{-1}) for a number of MCP stages are given in Table 1 and in Fig. 2, *b*. The spectral behavior of the coefficient $\Delta\varepsilon_0''$ is shown in Fig. 4 for the initial stage of the MCP, from which it can be seen that the main differences are observed in the vicinity of the antisymmetric oscillation $\nu_{as} \approx 1120$ cm^{-1} of the Si−O−Si bridge.

There are two more intense bands in the spectrum of SiO$_2$ quartz glass: $\nu_s \approx 800$ cm^{-1} is symmetric vibration, it is associated with the displacement an O atom in the Si−Si perpendicular direction in the Si−O−Si plane; band $\nu_\delta \approx 470$ cm^{-1} and is deformation vibration O−Si−O, this
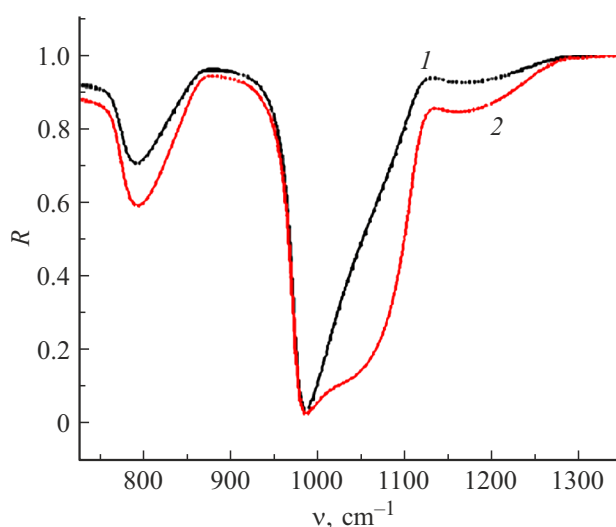

Figure 3. ATR spectra of KU-1 glass in the 1120 cm^{-1} band, MCP method; ATR element ZnSe, $N = 1$, $\theta = 73°$, polarization type: *1* — *s* , *2* — *p* . The sample was placed in optical contact with the ATR element.
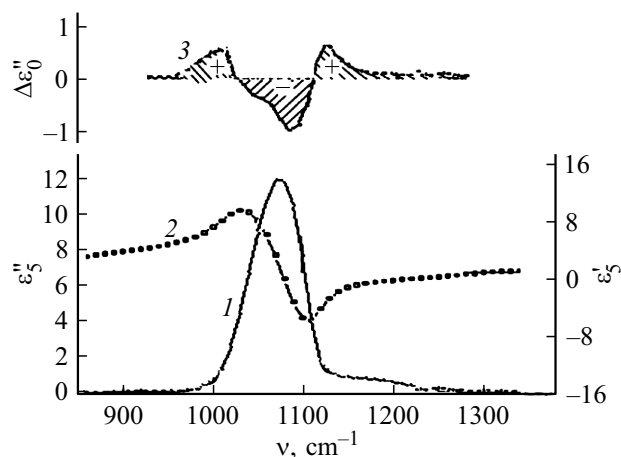

Figure 4. Spectral dependences of the dielectric functions of KU-1 glass: *1* — ε_5''; *2* — ε_5'; *3* — $\Delta\varepsilon_0''$ ($z_0 = 180$ nm).

frequency is also attributed to the rotational mode in the Si− bridge O−Si caused by displacement of the O atom outside the Si−O−Si [28,49] plane. In the vicinity of the long-wavelength bands 800 and 470 cm^{-1}, the amplitude changes in the R coefficient are less pronounced than for the 1120 cm^{-1} band, so the calculation of the value of $\Delta\varepsilon_0''$ for this frequency range gives a large error. The nature of this R dependence is associated with a decrease in the d_4/λ ratio as the wavelength increases. The function $\Delta\varepsilon_0''$ (Fig. 4) is characterized by extrema with ?+? sign in the region ≈ 1000 cm^{-1} and ≈ 1250 cm^{-1}. The nature of the coefficient $\Delta\varepsilon_0''$ for the frequency ≈ 1000 cm^{-1} is associated with the breaking of the bond in the Si−O−Si bridge and the formation of Si−OH groups and Si−O. The formation of these groups in the SL of KU-1 glass leads

to the appearance of characteristic bands for Si−O and Si−OH bonds in the regions $\approx 1000\,\mathrm{cm}^{-1}$ and $\approx 950\,\mathrm{cm}^{-1}$ respectively [50–52].

The increasing of the $\Delta\varepsilon_0''$ coefficient for the neighborhood $\nu_{as} \approx 1250\,\mathrm{cm}^{-1}$ (main strip shoulder $1120\,\mathrm{cm}^{-1}$) can be related to the increase in the number „of straightened" Si−O−Si bridges with angles $160–180°$ and the shortest and strongest bonds [25]. The weakening of the band $\nu_{as} \approx 1120\,\mathrm{cm}^{-1}$, which refers to bridges with normal connections, is associated with a redistribution between the number of loaded and unloaded bridges Si−O −Si. Tensile stresses in the SL affect the vibrational characteristics of the Si−O−Si bridges, which shifts the band $\nu_{as} \approx 1120\,\mathrm{cm}^{-1}$ to the low-frequency region of the spectrum [25,53].

The normal, least strained bonds of the Si−O−Si bridge in quartz glass have angles of $140–160°$ and length $\approx 1.60\,\text{Å}$, while elongated strained bonds are characterized by angles $\approx 120°$ and large length $\approx 1.68\,\text{Å}$ Si−O [25] bonds. The energy of such bonds is reduced by $20–30\%$ of the average energy for normal Si−O bonds in glass. The process of traditional MCP is closely related to the formation of local mechanical defects and cracks in glass, followed by the diffusion of H_2O molecules into the SL of the glass. Local defects in SL lead to bond stress in the Si−O−Si bridges and their hydrolysis upon interaction with water. It is on such bonds that the so-called „mechanically stimulated hydrolysis" occurs with the formation of Si−OH [25] groups. The MCP process using a high-hardness abrasive (diamond) and a habit of diamond microcrystals in the form of a sharp edged octahedron leads to a large number of local defects in the SL structure of glass KU-1. The mechanism of the MCP process with the help of diamond pastes is considered in the work [54].

The presence of Si−O and Si−OH groups in SL contributes to an increase in n; the concentration of such groups, based on the ratio of $\Delta\varepsilon_0''$ and ε_5'' (Fig. 4), is equal to $C \approx 3.6\,\mathrm{vol.\%}$. The close value of the desired value C gives a direct method for calculating the concentration of H_2O (hydroxyls) in SL by determining the intensity of the band $3650\,\mathrm{cm}^{-1}$, which is superimposed on the main band $3400\,\mathrm{cm}^{-1}$.

This band refers to molecular water on the surface of KU-1 glass. Calculations of the value of C by the described method were carried out on the basis of the ATR spectrum of water (Fig. 5) using equation (5), taking into account the relation $\alpha_4 = \varepsilon^0 C_{OH}$. The concentration $C \sim \Delta\varepsilon_0''$ decreases linearly with increasing SL depth (Fig. 6). A similar linear dependence is observed in the photoluminescence spectra [38] for the distribution of oxygen defects in SL:oxygen vacancy defects (ODC are Oxygen Deficient Centers) and non-bridging oxygen defects (NBOHC are non-bridging oxygen hole centers (Fig. 6)) Nonbridging oxygen defects fluoresce at a wavelength of $\lambda \sim 650\,\mathrm{nm}$, and oxygen vacancies fluoresce at $\lambda \sim 440\,\mathrm{nm}$.

Since the concentration of Si−O and Si−OH groups in the SL of quartz glass can reach $C \leq 6\,\mathrm{vol.\%}$ [25], and the refractive index of silicon monoxide (SiO) for $\lambda = 632.8\,\mathrm{nm}$

is equal to 1.96507 [55], then the presence of SiO and Si−OH in SL can explain the high value of n SL of glass for MCP. The gradient distribution of the parameter $C(z)$, which is characteristic of the initial stage of MCP, leads to a decrease in the value of n as the value of d_4 decreases during polishing up to the values of n in the bulk of the glass (Fig. 2, a and Table 1).

As an example of the effect of SL on the results of measurements of the reflection R and, accordingly, on the calculation of the optical parameters of quartz glass [47,56], the data of independent measurements (different polishing process) are given (Fig. 7, a), from which one can see a noticeable excess of R values in the region $900–1000\,\mathrm{cm}^{-1}$
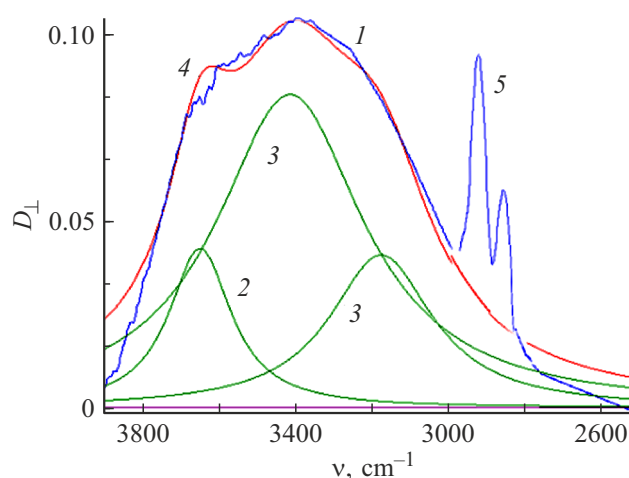
Figure 5. Optical density in the vicinity of the valence band H_2O and C_xH_y, ATR element SiO_2, $N = 100$, $\theta = 45°$, MHP method: *1* — experiment, *2* — ν_s band of hydroxyls in SL — $3650\,\mathrm{cm}^{-1}$, *3* — $\nu_{as,s}$ bands of molecular water: 3400 and $\approx 3180\,\mathrm{cm}^{-1}$, *4* is the total curve of decomposition of the strip *1* into individual components with a Gaussian contour, *5* are the bands $\nu_{as,s}$ of sorbed hydrocarbons C_xH_y.
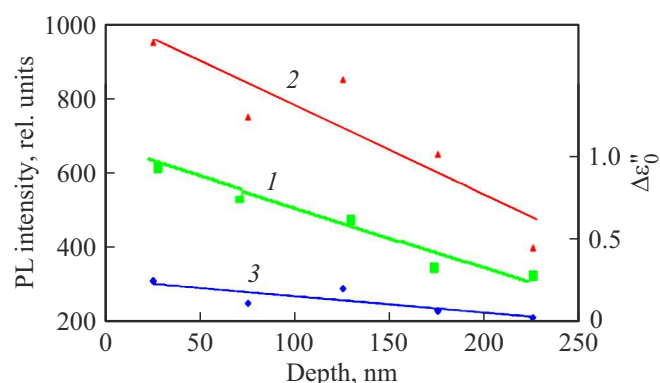
Figure 6. Dependence of the defect concentration in KU-1 glass on the SL depth, MCP method. *1* — $\Delta\varepsilon_0''$ ($\nu = 1000\,\mathrm{cm}^{-1}$) is proportional to the concentration of Si−O and Si*groups*−ON. For comparison, the intensity dependences of the $\lambda \sim 440$ and $\lambda \sim 650\,\mathrm{nm}$ photoluminescence bands are shown (proportional to the concentration of oxygen defects in 2-ODC and 3-NBOHC, respectively) [38].
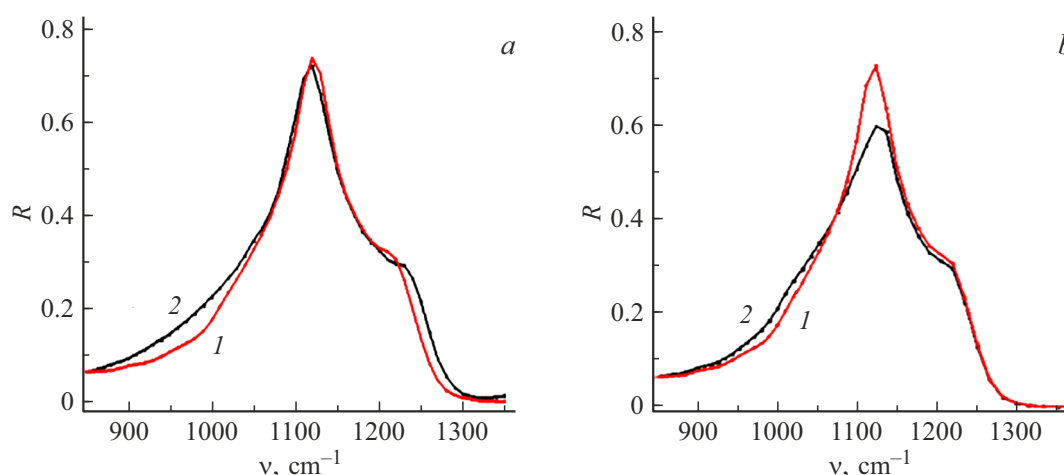
Figure 7. IR reflection spectra R of KU-1 glass near the normal in the band $\nu = 1120\,\text{cm}^{-1}$, MCP method: (*a*) calculation of R from $ndata(\nu)$ and $k(\nu)$: *1* — [56], *2* — [47]. (*b*) calculation of R for the system: layer composition $25 \cdot \text{SiO} - 75 \cdot \text{SiO}_2$-substrate SiO_2; layer thickness d: *1* — 0 nm, *2* — 120 nm. The optical properties $n(\nu)$ and $k(\nu)$ of the model?s SL are obtained using the Lorentz-Lorentz equation for the mixture $25 \cdot \text{SiO} - 75 \cdot \text{SiO}_2$.

and a slight decrease in R of the maximum of the $1120\,\text{cm}^{-1}$ band for the spectrum *2* with respect to the spectrum *1*.

The increase in the R value on the low-frequency wing of the $1120\,\text{cm}^{-1}$ band is due to the greater thickness and/or concentration of the Si−O and Si−OH groups in the SL of the polished glass sample for the spectrum *2* (Fig. 7, *a*). Model calculation of the R value for the film?s system of structure $25 \cdot \text{SiO} - 75 \cdot \text{SiO}_2$ on a SiO_2 substrate (Fig. 7, *b*) at a qualitative level allows confirming the presence of an increased concentration of SiO in the SL for the sample (Fig. 7, *a*, spectrum *2*). It can be noted that the R spectrum (band $1120\,\text{cm}^{-1}$) of quartz glass undergoes similar qualitative changes in a humid air atmosphere under the influence of a mechanical load on a thin plate of KU-1 glass when it is stretched with a force of 90 Pa [25].

The analysis of the properties of the SL formed as a result of MCP within the framework of the optical model (Fig. 1, *b*) correlates well with the results of the structural-morphological model (Fig. 1, *c*), which is formed on the basis of comprehensive research [38]. As a result of these studies, it was shown that under the fractured layer there is a defective layer at a depth from ~ 20 to $\sim 360\,\text{nm}$. This layer contains two types of defects: oxygen deficient centers and non-bridging oxygen hole centers at a depth of $\sim 20-250\,\text{nm}$ and high-density nanoparticles of unknown nature, the number of which decreases exponentially with increasing SL depth. At a depth from ~ 250 to $\sim 360\,\text{nm}$, the number of nanoparticles is insignificant, and the content of both types of oxygen centers continues to decrease until it becomes below the level that can be reliably detected by analyzing the fluorescence spectra. At a depth of more than $\sim 360\,\text{nm}$, a fused quartz matrix appears, which contains only some clusters of internal material defects.

The totality of the above information indicates a relationship between the presence of Si−O and Si−OH groups in
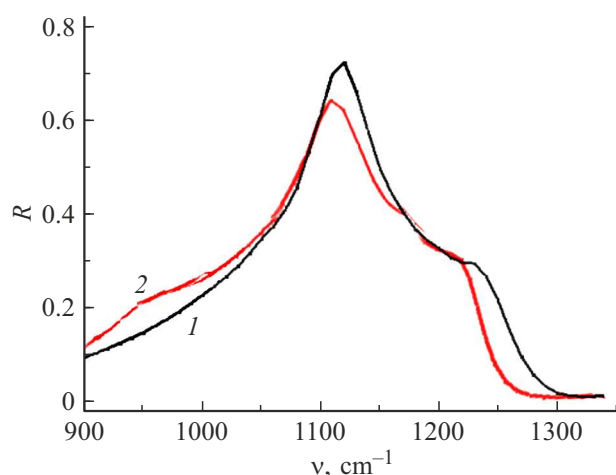
fused silica SL with the formation of oxygen centers. High-density nanoparticles are structural groups in the form of clusters formed by Si−O−Si defect bridges, the configuration of which is different from the corresponding matrix bridges. The presence of such structural formations in the SL of fused quartz is confirmed by Raman spectroscopy data, where additional bands were found: the peak $D1$ — $490\,\text{cm}^{-1}$ is attributed to the in-phase respiratory motion of oxygen atoms in four-membered corrugated ring structures, and the peak $D2$ — $605\,\text{cm}^{-1}$ is associated with in-phase respiratory movements of oxygen atoms in planar three-membered ring structures [25]. Quartz glass contains about 1% of 3- and 4-membered rings, while in the less equilibrium structure that occurs in SL, their concentration is noticeably higher than in the volume of the glass. The Si−O bonds in these rings are elongated compared to those typical for a glass network and are in a stressed state. Selective hydrolysis of Si−O bonds during MCP of glass occurs on such strained ring structures [25]. The results presented indicate the similarity of the chemical composition of the SL formed by different technological methods of MCB of quartz glass and allow us to explain the main reason for the variation in the values of the optical constants determined from the reflection spectra

Focused ion beam polishing

The focused ion beam polishing was originally used to remove the fractured layer and improve the surface microrelief after MCP [32−36,57−59]. The removal of a defective surface layer by IBB makes it possible to obtain surfaces that are close in chemical composition and structure to the properties of the material in the bulk, which improves light transmission in the UV and increases the radiation strength of the optical element. Subsequently, the

Table 2. Optical characteristics of SL for different methods of polishing KU-1 and K-8 glasses according to ellipsometry and IR spectroscopy data

Characteristics of SL	MCP	IBB, Ar$^+$			
	KU-1	KU-1		K-8	
		0.5 keV	1.5 keV	0.5 keV	1.5 keV
$N_{el}(\lambda = 632.8\,\text{nm})$	1.462 [42]	1.480	1.484	1.542 [35]	1.545 [35]
$N_{ir}(\nu \approx 1100\,\text{cm}^{-1})$	1.406 [46]	1.580	1.621 [33]	1.558	1.579
	1.445 [55]				
	1.435 [27]				
	1.510 [48]				
$D_{el}(\lambda = 632.8\,\text{nm})$, nm	200 [42]	10	15	55 [33]	230 [33]
$D_{ir}(\lambda = 8\,\mu)$, nm	180 [42]	12.5	21	62	240
$R\%(\nu = 1120\,\text{cm}^{-1})$	73.5 [27]	71.5	69	32.2	29.0
$\Delta\varepsilon_0''(\nu = 1250\,\text{cm}^{-1})$	0.54 [42]	0.56	0.60	0.34	0.36

Figure 8. IR reflection spectrum R of KU-1 glass near the normal in the band $\nu = 1120\,\text{cm}^{-1}$, IBB method: Ar$^+$ ion beam with energy: *1* is 0.5, *2* to 1.5 keV.

ion processing method found application in works on the shaping of optical surfaces [33,34,36].

The physical foundations of the BIP polishing process are described in the works [29–34]. In the framework of this work, to interpret the results, it suffices to rely on a simplified scheme for the transfer of excitation energy from an ion with energy E to atoms of the target structure. As a result of the transfer of energy E from the ion to the atoms, the target atoms in the surface layer are excited, the value of which corresponds to the twofold penetration depth of the ion into the target $(2-10\,\text{nm})$. On real optical surfaces that have undergone preliminary MCP, the value of the SL formed under vacuum conditions during the IIP is much larger. At excitation energies above $\approx 0.5\,\text{keV}$, some of the atoms are removed from the target SL, and the structure of this layer is destroyed As a result of ion bombardment, oxygen vacancies appear in SL and broken interatomic bonds are formed. Strained configurations with elongated

Si−O bonds and angles $\approx 120°$ begin to predominate in the distribution of Si−O−Si bridge types in the SL of quartz glass, which makes the surface chemically active. Therefore, after ion bombardment of the target in vacuum and subsequent removal of the sample from the chamber, the surface will actively interact with the external medium (usually air) and, accordingly, the properties of such a surface will depend on the composition of the gases of the external medium.

SL properties for the IIP method were actively studied using ellipsometry [32–35], which made it possible to study the properties of SL, including the refractive index, thickness and height of SL microroughnesses for quartz glass and a number of multicomponent glasses [32–35] . The use of a complex of modern methods: atomic force and electron microscopy, luminescence, IR and Raman spectroscopy, mass spectroscopy, etc., made it possible to study in detail the properties of SL at the atomic and molecular level [36–39,57–59]

In the present work, the main attention is paid to the study of the structure of the SL of KU-1 quartz glass formed upon ion bombardment. Spectrum of KU-1 glass after processing[2] by beam of Ar$^+$ ions with energy 0.5 and 1.5 keV is shown in Fig. 8.

It can be seen from the figure that an increase in the energy of Ar$^+$ ions reduces the intensity of the main band $1120\,\text{cm}^{-1}$ and leads to an increase in the low-frequency wing i.e. the region $900-1000\,\text{cm}^{-1}$.

Similar transformation of the band $1120\,\text{cm}^{-1}$ also occurs for MCP processing of KU-1 glass (Fig. 7, a). The data obtained for two IBB regimes (E of Ar$^+$ ions 0.5 and 1.5 keV) of KU-1 and K-8 glasses are summarized in Table 2.

It can be seen from the table that for the IBB mode 0.5 keV, the thickness, refractive index, and dielectric loss $\Delta\varepsilon_0''$ for the SL of KU-1 glass are smaller than for the

---

[2] Ion processing of KU-1 samples was performed at the Vavilov's State Optics Institute in the Perveev?s laboratory.

1.5 keV mode. At the same time, the value of the IR reflection R in the band $\nu = 1120\,\text{cm}^{-1}$ and the loss $\Delta\varepsilon_0''$ ($\nu = 1250\,\text{cm}^{-1}$) of KU-1 glass for the BIP method is higher for 0.5 keV in comparison with the 1.5 keV mode, but somewhat lower than for the IBB method. The totality of the data in Table 2 shows that during the processing of KU-1 glass by the IBB method for the mode 1.5 keV, the concentration of defects in the glass network structure in the SL, including the Si−O and Si−OH groups, is higher than for the method MCP, however, the thickness of the SL for IBB is somewhat lower compared to MCP.

The study of the SL of quartz glass by Raman spectroscopy shows that, as a result of bombardment with Ar$^+$ ions, deformed Si−O−Si bridges with strained bonds appear in LS. These bonds form structural ring formations: peak D1 — 490 cm^{-1} and peak D2 — 605 cm^{-1}, in 4- and 3-membered ring structures, respectively [59]. The relative intensities of the $D1$ and $D2$ peaks initially increase when the ion beam etching depth is 50 nm, which indicates the removal of coarse nanosized structural defects in the SL and the increase in the degree of compaction compared to the initial surface. The relative intensities of the $D1$ and $D2$ peaks gradually decrease with increasing SL depth. With the help of the IBB method, the number of structural defects can be significantly reduced without compromising the surface quality of the fused quartz. As a result of the action of the IBB, the photothermal absorption of the fused quartz surface can, according to various estimates, be reduced by a factor of 1.5−2, and the laser-induced breakdown threshold can be increased by a factor of 2 or more. The main structural transformations in the SL of quartz glass for the IBB method are in many respects similar to those transformations that are observed for the MCP method.

Conclusion

The conducted studies show that the structural and chemical features of the SL of fused quartz, which are formed during its processing by the MCP and IBB methods, are largely similar and are associated with deformation and breaking of bonds in the Si−O−Si bridges of the glass network. For MCP method, the hydrolysis mechanism for rupture of strained molecular bonds is realized, and for IBB method, is realized he mechanism of energy action on the bonds of the glass network is realized The use of at the final stage of the MCB improves the characteristics of SL, making it possible to reduce its thickness and thereby increase the UV light transmission and laser breakdown threshold of fused silica. According to the data obtained, one can expect an additional improvement in the corresponding parameters when using IBB method with a decrease in the energy of the ions acting on the object in the final stage of processing.

References

[1] Lord Rayleigh. Proc. Royal Soc. London A, **60**, 507 (1937).
[2] I.V. Grebenshchikov. Izv. AN SSSR. Sektsiya tekhn. nauk, (1), 3, (1937).(In Russian)
[3] N. Kachalov. *Osnovy protsessov shlifovki i polirovki stekla* (Publ. house AS of the USSR, M., 1946) (in Russian)
[4] A. Adamson. *Fizicheskaya khimiya poverkhnostey* (Mir, Moscow, 1979) (in Russian)
[5] T.N. Krylova. Vavilov State Optical Institute **45** (179), 47, (1979) (in Russian)
[6] E.Ya. Goz, R.S. Sokolova, A.Ya. Kuznetsov. OMP, (12), 69 (1969). (in Russian)
[7] J.G. Smith, J. Hooley. Canadian J. Technol., **31** (2/3), 37 (1973).
[8] A. Kuller. Silicattechnik, **7** (10), 380 (1956).
[9] G.O. Rawstron. J. Soc. Glass Technol., **42**, 253 (1958).
[10] H. Komogava. Proc. Phys. Math. Soc. Japan, **8**, 384 (1943).
[11] S. Harada, T. Isumitani. Glass Technol., **12** (5), 131 (1971).
[12] H. Sakata. Verres Refract, **12** (2), 58 (1973).
[13] J.P. Mariage. Neuv. Rev. Optique, **6** (2), 121 (1975).
[14] Y. Yokota, H. Sakata, M. Nishibori, K. Kinosita. Surf. Sci., **16**, 265 (1969).
[15] A.E. Chmel, V.I. Vettegren, K.N. Kuksenko. In: *Opticheskiye i spektral'nyye svoystva stekol* (abs. 3rd All-Union. sympos., State Optical InstituteI, Leningrad, 1974), pp. 45−46, (in Russian).
[16] V.I. Pshenitsyn, N.Kh. Holdarov, I.A. Khramtsovsky, M.A. Kalinina, N.I. Tikhomirova. OMP, (8), 28 (1987). (in Russian)
[17] V.I. Pshenitsyn, G.T. Petrovsky, V.N. Stepanchuk. In: *Nerazrushayushchiye fizicheskiye metody i sredstva kontrolya* (abs. 9th All-Union. scientific and technical Conf., Minsk, May 26−28, 1981), p. 161 (in Russian)
[18] H. Fukyo, N. Oura, N. Kitajiama, H. Kono. J. Appl. Phys., **50** (5), 3653 (1979).
[19] J.C. Channet, P.G. de Gennes. J. Opt. Soc. Am., **73** (12), 1777 (1983).
[20] L.L. Vasilyeva, K.K. Svitashev, A.I. Semenenko, L.V. Semenenko, V.K. Sokolov. Opt. i spektr., **37** (3), 574 (1974) (in Russian).
[21] Z. Gu, P. Liang, W. Zhang. Optical Engineering, **41** (7), (2002). DOI: 10.1117/1.1480426
[22] I.H. Malitson. JOSA, **55**, 1205 (1965).
[23] A.I. Semenenko. Nauch. priborostr., **15** (2), 88 2005 (in Russian)
[24] G.M. Mansurov, R.K. Mamedov, A.S. Sudarushkin et al. Opt. i spektr., **52** (5), 852 (1982) (in Russian).
[25] V.A. Bershteyn. *Mekhano-gidroliticheskiye protsessy i prochnost' tverdykh tel* (Nauka, Leningrad, 1987) (1982) (in Russian).
[26] A.M. Efimov, V.G. Pogareva, V.N. Parfinskii, M.A. Okatov, V.A. Tolmachev. Glass Technology, **46** (1), 20 (2005).
[27] V.M. Zolotarev. Opt. i spektr., **107** (5), 794 (2009) (in Russian).
[28] R. Kitamura, L. Pilon, M. Jonasz. Appl. Opt., **46** (33), 8118 (2007).
[29] G. Carter, J.S. Colligon. *Ion Bombardment of Solids* (Amer. Elsevier Pub. Co., N.Y., 1968).
[30] P. Sigmund. *Raspyleniye tverdykh tel ionnoy bombardirovkoy* (Mir, Moscow, 1984) (in Russian)

[31] P. Sigmund. Phys. Rev., **187**, 768 (1969).
DOI: 10.1103/PhysRev.184.383

[32] A.F. Perveev, A.V. Mikhailov, V.V. Ilyin. OMP, (10), 40 (1972).(in Russian)

[33] A.F. Perveyev, L.V. Vishnevskaya, L.A. Cherezova. *Ionnaya obrabotka opticheskikh materialov i pokrytiy* (NTTS „Informatika", Moskva, 1990) (in Russian)

[34] L.A. Cherezova. Optich. zhurn., **67** (10), 1 (2000) .(in Russian)

[35] I.A. Khramtsovsky, T.K. Voshchenko, L.A. Cherezova, V.I. Pshenitsyn, A.A. Apinov. Opt. i spektr.,**65** (1), 141 (1988) (in Russian).

[36] N.I. Chkhalo, S.A. Churin, M.S. Mikhaylenko et al. Appl. Opt., **55** (6), 1249 (2016). DOI: 10.1364/AO.55.001249

[37] A. Keller, S. Facsko, W. Moller. J. Phys.: Condens. Matter, **21**, 495305 (2009). DOI: 10.1088/0953-8984/21/49/495305

[38] Y. Zhong, F. Shi, Y. Tian, Y. Dai, C. Song, W. Zhang, Z. Lin. Opt. Expr., **27** (8), 10826 (2019).
DOI: 10.1364/OE.27.010826

[39] P.E. Miller, T.I. Suratwala, L.L. Wong, M.D. Feit, J.A. Menapace, P.J. Davis, R.A. Steele. *In: Laser-Induced Damage in Optical Materials* (Proc. SPIE, 5991, 2005).
DOI: 10.1117/12.638821

[40] N.N. Rozanov, V.M. Zolotarev. Opt. i spektr., **49** (5), 925 (1980) (in Russian).

[41] G.M. Mansurov, N.N. Rozanov, V.M. Zolotarev, S.M. Sutovsky. Opt. i spektr., **53** (5), 301 (1982) (in Russian).

[42] V.M. Zolotarev. *Issledovaniye svoystv materialov v ob"yeme i surface layer by methods of internal reflection spectroscopy* (Vavilov State Optical Institute, Leningrad, 1981) (in Russian).

[43] E.D. Palik, R.T. Holm. Optical Eng., **17** (5), 512 (1978).

[44] N.J. Harrick. *Internal Reflection Spectroscopy* (Wiley, NY, 1967).

[45] I.M. Minkov, E.L. Velitskaya, V.M. Zolotarev, L.N. Kapitonova. Opt. i spektr., **58** (689) (1995) (in Russian).

[46] S.S. Gusev, N.I. Staskov, V.V. Filippov. Opt. i spektr., **49** (1), 117 (1980) (in Russian).

[47] *Handbook of Optical Constants of Solids*, ed. by E.D. Palik (Acad. Pr., NY, 1985).

[48] V.M. Zolotarev, V.N. Morozov, Ye.V. Smirnova. *Opticheskiye postoyannyye prirodnykh i tekhnicheskikh sred* (Khimiya, Leningrad, 1984) (in Russian).

[49] A.M. Efimov. *Optical Constants of Inorganic Glasses* (CRC Press, Boca Raton, 1995).

[50] L. Alipour, S. Nakashima. Appl. Spectr., **70** (3), (2016).
DOI: 10.1177/0003702815626665

[51] Fu Huiqin, Ding Xingeng et al. RSC Adv., **7** (27), 16264 (2017). DOI: 10.1039/C6RA27219C

[52] S. Wetzel, M. Klevenz, H-P. Gail et. al. A & A, **553** (A92), 1 (2013). DOI: 10.1051/0004-6361/201220803

[53] M. Tomozawa, Y-K. Lee, Y-L. Peng. J. Non-Cryst. Sol., **242** (2−3), 104 (1998).

[54] V.I. Kurban', T.T. Skripko et all Sinteticheskiye almazy, (3), 5 (2001) (in Russian).

[55] M. Polyanskiy. Refractive Index. INFO website: 2008−2022 (Electronic source) https://refractiveindex.info/

[56] T.R. Steyer, K.L. Day, D.R. Huffman. Appl. Opt., **13**, 1586 (1974). DOI: 10.1364/AO.13.001586

[57] A.I. Stogniy, H.H. Novitskiy, O.M. Stukalov. Pisma v ZhTF, **28** (1), 39 (2002) (in Russian).

[58] N.N. Andrianova, A.M. Borisov, V.V. Borovskaya. Prikl. fizika, **2**, 36 (2012). (in Russian).

[59] Y. Zhong, Y. Dai, F. Shi, C. Song, Y. Tian, Z. Lin, W. Zhang, Y. Shen. Materials, **13** (6), 1294 (2020). DOI: 10.3390/ma13061294